Rev. Adv. Mater. Sci. 31 (2012) 100-108

KINETIC MODELLING OF FLOW STRESS OF METALS AND ALLOYS PROCESSED BY SEVERE PLASTIC DEFORMATION

R.G. Chembarisova, M.I. Latypov and I.V. Alexandrov

12, Karl Marx, Ufa State Aviation Technical University, Ufa, 450000, Russia

Received: April 20, 2012

Abstract. Basing on the kinetic modeling, the quantitative evaluations of activity of mechanisms, affecting the strength properties to explain the deviations from the Hall-Petch law towards the greater side in the area of small grains, have been made. The income of each strengthening mechanisms has been evaluated. It has been shown that the grain size and the pinning of dislocations by Mg atoms in the grain boundaries area are the main factors that enhance the alloy strength. The obtained results can be helpful for predicting the mechanical properties of materials.

1. INTRODUCTION

Understanding of the mechanisms that determine deformation behavior of metals and alloys as their control is a topical issue. The correlations describing plastic deformation behavior of metallic materials are built on the basis of dislocation conception. Static and dynamic experiments are effectively described from the point of view of the kinetic approach. This approach is based upon the investigation of inner microscopic processes that take place in metals and alloys during their deformation and control their non-elastic behavior with contribution of dislocations, as well as the other, in particular, point defects of a crystal lattice. Thus, the processes of emission, further movement and annihilation of dislocations are taken into consideration. Presently, there are plenty of experimental data for determination of dislocation density, rate and geometry of their slip, concentration of point defects [1, 2], which can be used in modeling.

Kinetic modeling allows considering the properties of a certain material suffering the plastic flow. Herein, the comparison of the modeling results and corresponding experimental data allows determining the kinetic parameters involved into analytical correlations.

The kinetics of dislocations and point defects described in terms of average parameters, characterizing their evolution on the microscopic level, is connected with macroscopic parameters that characterize the environment behavior on the whole. In paper [3] Taylor considered the plastic deformation as the result of dislocation movement, while strengthening is the result of dislocation density increase due to their multiplication and the following locking by the obstacles of dislocation origin. From the Cottrell's point of view [1], impurity atoms lock dislocations as well, which leads to additional material strengthening.

Recently, the kinetic approach has been frequently used in respect to metallic materials subjected to severe plastic deformation (SPD) to analyze the mechanisms operating in deformation strengthening and to explain the peculiarities of deformation behavior of bulk ultrafine-grained (UFG) materials [4-7]. The plastic behavior of metals and

Corresponding author: I.V. Alexandrov e-mail: iva@mail.rb.ru

alloys is investigated in a wide range of deformation rates and temperatures. The principle models applied to solve the assigned problems are the upgraded models of Estrin-Tóth and Zehetbauer [8-11], which can be useful for predicting material properties during their exploitation.

It is a common knowledge that the strengthening properties of materials can be varied by structure refinement, dynamic ageing, precipitation of particles of the 2nd phase, segregations of atoms along the grain boundaries (GBs). For instance, the authors of the papers [5,12] have obtained high values of yield stress in the Al 1570 (Al–5.7Mg–0.32Sc–0.4Mn, wt.%) and Al 6061 (Al–1.0Mg–0.6Si–0.3Cu–0.25Cr–0.15Mn–0.7Fe–0.25Zn–0.15Ti, wt.%) alloys subjected to high pressure torsion (HPT) at room temperature (RT). During the experimental research of the structure of Al alloys, subjected to SPD and showing fair (in case of the Al 6061 alloy) or very high (in case of the Al 1570 alloy) strength, the deviations from the Hall-Petch (HP) law have been revealed [13,14]. Thus, the segregations have been found along the GBs. The authors of the works [5,12] reasonably assign a key part to segregations in developing the ultra-high-strong states mentioned above. The same factors can be responsible for the development of a super-strong state in Ti, which have been demonstrated by the authors of the paper [15] on the examples of Ti Grade 4 samples (Ti – base, C – 0.052, O – 0.34, Fe – 0.2, N – 0.015, wt.%).

In the present work on the Al 1570 alloy example quantitative evaluations of activity of mechanisms affecting the strength properties have been made to explain the deviations from the HP law towards the greater side in the area of small grains.

2. THE MODELING CONCEPT

2.1. Strengthening mechanisms

2.1.1. The superposition of strengthening mechanisms

The following strengthening mechanisms are considered to be operating in the alloys: work hardening τ_p, solution hardening τ_c [16], precipitate hardening τ_f [17], lattice friction τ_0 (the power of Peierls-Nabarro [2,18]). These mechanisms interact with each other in a certain way. Their combination may be simple as well as complicated, when each mechanism has an effect on others. Various rules of superposition are mentioned in literature [16,19]. The most common and simple one is the linear addition

$$\tau = \sum \tau_i, \tag{1}$$

where τ is the overall flow stress or the yield stress, τ_i is contribution of *i*-th mechanism.

The linear sum provides a good approximation with a small number of hard obstacles as well as with a large number of soft obstacles in the material. In the present model the simplest linear addition will be assumed as good approximation. That is because, for example, the lattice friction and solute obstacles are acting along the whole dislocation line, while a dislocation moves in the crystal lattice.

The equivalent single-axis flow stress σ of a polycrystal was derived from the theoretical critical resolved shear stress τ in order to compare the latter with the experimental yield stress obtained by tensile tests. In order to do that, the following general expression is used [16]:

$$\sigma = M\tau, \tag{2}$$

where *M* is the constant called the Taylor's factor. In this paper a value of 3.07 is assumed for the Taylor's factor [19].

The plastic deformation is determined according to the dislocation conception. That is why a well-known correlation between the flow stress τ_p, conditioned by the dislocation interaction with each other, and the dislocation density ρ_{tot} [19,20] has been used in the developed model:

$$\tau_p = \alpha G b \rho_{tot}^{1/2}, \tag{3}$$

where α – the coefficient, considering the thermal activation of dislocation interaction, *G* – the shear modulus, *b* – the Burgers vector. In this case increase in the flow stress during deformation is due to dislocation accumulation. The HP relation within the framework of the classical model of work hardening results from this relationship for coarse-grained (CG) materials.

Work hardening of crystalline material determined by dislocation-dislocation interaction is given by the Taylor's relationship (3). This relationship accounts change in the average dislocation density due to dislocation generation, multiplication and annihilation during plastic deformation [1,18,21,22]. In metallic materials dislocations interact with each other during their motion as well as with other lattice defects that retard dislocation motion. Dislocations need an additional input of energy for further advance, and this results in work hardening.

The present model was constructed basing on most probable hardening mechanisms that were

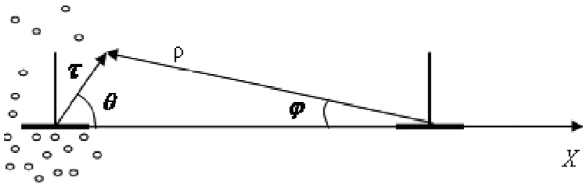

Fig. 1. The location of atoms in a frozen solute atmosphere in relation to the displaced dislocation are characterized by the radius-vector ρ and the angle φ.

determined according to experimental data concerning microstructure of aluminum alloys.

2.1.2. The dislocation pinning by atmospheres of impurity atoms

The edge dislocation is surrounded by the Cottrell atmosphere from the solute atoms [1]. Bonding energy of a positive edge dislocation with an impurity atom in a simple case of purely hydrostatic interaction is equal to work due to inserting a solute atom of radius R_S instead of a matrix atom of radius R_a that results in a volume change $dV = 4\pi(R_s^3 - R_a^3)/3$ at the point with coordinates (Θ,r) under local pressure $P = \sigma_{ii}/3$:

$$W = P(\Theta,r)\,dV. \qquad (4)$$

The individual volume of an impurity atom is so small, that it is possible to assume that $P = const$. Considering the components of stress tensor σ_{ij} for the edge dislocation, it is possible to accept the following:

$$P = \frac{1+\nu}{1-\nu}\frac{\sin\Theta}{r}\frac{Gb}{3\pi}. \qquad (5)$$

Taking into account the only linear component $\varepsilon = (R_S - R_a)/R_a$ in the Taylor series expansion, one can assume the excess volume as $dV = 4\pi R_a^3\varepsilon/3$. As a result, the interaction energy is expressed as:

$$W = \frac{4}{9}R_a^3\varepsilon\frac{1+\nu}{1-\nu}\frac{\sin\Theta}{r}Gb = \beta\frac{\sin\Theta}{r}. \qquad (6)$$

Here the coefficient

$$\beta = \frac{4}{9}R_a^3\varepsilon\frac{1+\nu}{1-\nu}Gb.$$

θ - is the angle between the radius-vector $\vec{r}$ and the direction of the dislocation slip x (Fig. 1).

In case of a substitutional solute atom, R_a is the radius of the matrix atom, in case of interstitial solution, it is the radius of a sphere that would not cause volume distortions in the solute atom site. The formula (6) has been obtained in suggestion of elastic interaction of dislocation with an impurity atom and cannot be used in the inner area of a dislocation core, where the theory of elasticity of continuous medium cannot be applied. The divergency in the area $r \to 0$ is excluded by introducing the dislocation core of the size of a few interatomic distances. However, referring to the gradient elasticity theory, which considers second derivatives from the strain tensor in the Hook's law and describes the stress fields allows reducing singularity at $r \to 0$.

Within the gradient theory the elasticity one gets abstracted from the atomic crystal structure, considering it as a continuous medium. To model the interaction of an edge dislocation with an impurity atom, the impurity atoms are considered to be the dilatation centers, and the dislocation line is considered as the dislocation model. The substitution of the traditional Hook's law, which is true in the linear elasticity theory, by its gradient modification allows reducing the divergences from the fields of elastic strains. This fact, in its turn, brings to their reduction from the relations for elastic energies of dislocations [23].

The characteristic length equal to $\approx 1.25a$, where a – is the parameter of a crystal lattice, directly appears in the gradient elasticity theory, which can be considered as the radius of dislocation core. This allows making calculations without a simulated introduction of the radius cutting of elastic field on the dislocation core and the separate consideration of the core energy.

The authors of the paper [23] derived expressions for stress fields of structural defects, the accounting of which brings to the change of expression for the interaction energy between the edge dislocation and an impurity atom [1,24]. Taking into consideration the components of a stress tensor in the gradient elasticity theory, the energy is given by

$$W = \beta\left[\frac{1}{r} - \frac{K_1\left(\frac{r}{\sqrt{s}}\right)}{\sqrt{s}}\right]\sin\Theta. \qquad (7)$$

The direction of the Burgers vector corresponds to the angle $\Theta = 0$. The gradient coefficient $\sqrt{s} \approx a/4$ for the edge dislocation. K_1 is the modified Bessel's function of the second type of the first order. The extreme value of dimensionless energy $W\sqrt{s}/\beta$ of interaction at $\Theta = 3\pi/2$ is achieved at

$r/\sqrt{s} \approx 1.115$. This extreme value is the least negative value corresponding to the maximum value of the bonding energy at $\Theta = 3\pi/2$. The substitution atoms with $R_S > R_a$ and all the interstitial atoms are attracted to the area under the edge of an extraplane.

Solute atoms adsorbed along dislocations increase the resistance of plastic deformation and strengthen the material [1,19]. A dislocation pinned by solute atmospheres requires increment in stress for its further motion. If such a stress σ_S cannot be reached, the dislocation becomes blocked and does not contribute to plastic deformation anymore. In both cases the strain resistance increases up to the break-off of this dislocation or up to multiplication of others [19].

An uniform distribution of concentration of the point defects surrounding the dislocation is described by the expression

$$c = c_0 \exp\left(-\frac{W}{kT}\right), \tag{8}$$

where k – the Bolzmann constant, c_0 - the concentration of impurity atoms at the distance from dislocation. During the dislocation motion from the fixed cloud to the distance x (Fig. 1), the total interaction energy of dislocation with the solute atmosphere W_c per unit length of the dislocation line is [1]

$$W_c = \beta \int_{r_0}^{\infty} \int_0^{2\pi} (c - c_0) \left[\frac{1}{\rho} - \frac{K_1\left(\frac{r}{\sqrt{s}}\right)}{\sqrt{s}} \right] \frac{r \sin\Theta}{\rho} r \, dr \, d\Theta, \tag{9}$$

where $\rho = \sqrt{r^2 + x^2 - 2rx\cos\Theta}$..

The stress per unit length required to displace a pinned edge dislocation by x is determined as a derivative from the bonding energy W per unit length of dislocation [1]

$$\tau_s b = \frac{F}{L} = \frac{\partial W}{\partial x}. \tag{10}$$

$$\frac{F\sqrt{s}}{L} = 4\beta c_0 \int_{r_0}^{\infty} \int_0^{\pi} sh\left[\frac{\beta}{kT} \left(\frac{1}{r} - \frac{K_1\left(\frac{r}{\sqrt{s}}\right)}{\sqrt{s}} \right) \sin\Theta \right] \times$$

$$\left\{ \frac{\sqrt{s} r^2 \sin\Theta (x - r\cos\Theta)}{(x^2 + r^2 - 2rx\cos\Theta)^2} - \frac{r^2 \sin\Theta (x - r\cos\Theta)}{x^2 + r^2 - 2rx\cos\Theta} \times Q(x) \right\} dr \, d\Theta, \tag{11}$$

$$Q(x) = \frac{K_0\left(\frac{\rho}{\sqrt{s}}\right)}{2\sqrt{s}} + \frac{K_1\left(\frac{\rho}{\sqrt{s}}\right)}{\rho},$$

where $K_0\left(\rho/\sqrt{s}\right)$ - is the modified Bessel's function of the second type of zero order, L – the length of dislocation.

So, considering all the hardening factors the flow stress or yield strength of aluminum alloys is given by

$$\tau = \tau_0 + \tau_c + \tau_f + \tau_s + \alpha G b \rho^{1/2} = \tau_d + \tau_s + \alpha G b \rho^{1/2}. \tag{12}$$

The friction stress τ_n during the interaction of moving dislocations with lattice defects and various obstacles of non-deformation origin is of the form:

$$\tau_n = \tau_0 + \tau_c + \tau_f + \tau_s = \tau_d + \tau_s. \tag{13}$$

The stress τ_c is conditioned by the changes in the values of the crystal lattice parameter and the elasticity modulus proportionally to the atomic impurity share [19].

Deriving the Peierls-Nabarro stress τ_0 is quite complicated. Calculations in literature for certain structures [1,2] are rather qualitative and do not provide precise values [25]. Thus, this value is determined as in work [26] by subtraction of other components of strengthening from the expression for determination of the yield strength.

Since it is hard to obtain the stress values τ_0, τ_c, and τ_f, a new term τ_d was introduced in expressions (12), (13). Multiplying by the Taylor's factor, this term is expressed as

$$\sigma_d = \sigma_0 + \sigma_c + \sigma_f. \quad (14)$$

The stress value σ_d has been estimated from the HP relation at $d^{-1/2} \to 0$ using experimental data on flow stress of the alloy. In the case of the alloy Al-Mg 1570 $\sigma_d \approx 220$ MPa (Fig. 2).

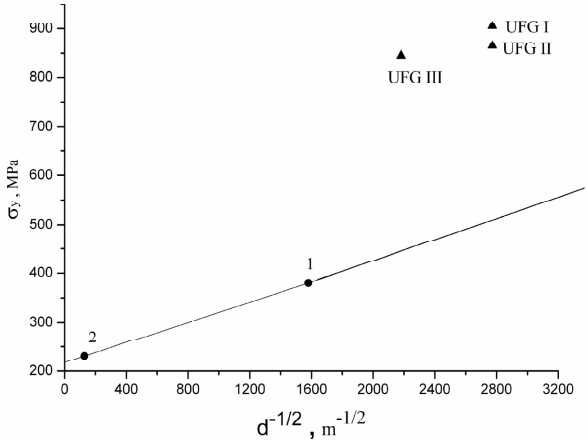

Fig. 2. The dependence diagram of the yield strength on the grain size in power -1/2. 1 – the yield strength of Al 1560 and 5083 alloys; 2 – the yield strength of a CG alloy 1570 without an additional hardening by Mg atoms located along the GBs, the colored triangles – the experimental values (Table 1).

2.2. The principal correlations of dislocation kinetics

2.2.1. The limit of free dislocation path

If the grain size influences mainly the average length of a free dislocation path, at a certain deformation degree γ the dislocation density ρ_{tot} in the material is proportional to the value, which is opposite to the average grain size d [9]:

$$\frac{d\rho_{tot}}{d\gamma} = \frac{1}{bCd}, \quad (15)$$

where C – the constant.

2.2.2. The deformation incompatibility

Besides the limitation of dislocation free path, the strain accommodation is the second reason that deformation behavior of a polycrystal differs from that of a single crystal [19]. Low plastic strains of a polycrystal start with independent dislocation slip in individual grains. In 40% of them slip is multiple from the very beginning [19]. Even in the case of a single slip the choice of the slip system is determined by the stress fields caused by incompatibility of elastic strains, not by the external stresses. Additional slip systems should act here for deformation accommodation in the boundary vicinity - the flow is getting complicated, and strain in each individual system is not uniform [19].

Accordingly, increase in the dislocation density in a polycrystal (due to the presence of GBs) is a result of GBs acting as barriers for dislocations and deformation incompatibility. According to work [22] dislocation accumulation due to the incompatibility could be described by the expression, which is similar to the expression (15). For this reason the following term has been inserted into the equation of dislocation density evolution to account the GBs' effect on the dislocation accumulation

$$\frac{d\rho^*_{tot}}{d\gamma} = \frac{\beta}{bd} \quad (16)$$

with the coefficient β that is determined basing on the experimental data.

2.2.3. Multiplication by the double cross slip

In the model the possible increase of dislocation density as a result of their multiplication by the double cross slip has been considered as well. Multiplication by double cross slip is described in details in monographs [1,19]. A dislocation loop formed by the cross slip in the plane parallel to the initial one and pinned by jogs acts as a Frank-Read source in the second plane. This is a significant way of dislocation multiplication, because the source appears as a result of dislocation slip.

There is distinct multiplication on the obstacles of deformation and non-deformation nature. In both cases the dislocation accumulation is determined by the free dislocation path:

$$\frac{d\rho^*_{tot}}{d\gamma} = \frac{1}{b\lambda_f} + \frac{1}{b\lambda_p}. \quad (17)$$

The length of the free path between obstacles of non-deformation origin (e.g. non-deformable precipitates) λ_P depends on the features of their distribution in the matrix such as size, volume fraction and spacing. The same factors determine precipitate hardening. For this reason, the following empirical relationship between the critical resolved shear stress due to precipitates and the mean free path presented in [22] was used

$$\frac{b}{\lambda_p} = (1-2)\cdot 10^{-2}\left(\frac{\tau_n}{G}\right). \tag{18}$$

It is known that sessile dislocations are effective barriers for slip dislocations (Lomer-Cottrell barriers) [18] and, hence, are also considered as obstacles, on which multiplication by cross slip can take place. The distance between the acts of cross slip λ_f was determined the same way as in work [22], according to the expression obtained according to the experimental data:

$$\lambda_f = \frac{1}{\delta_f \rho_f^{1/2}}. \tag{19}$$

where δ_f is the coefficient of dislocations multiplication on forest dislocations of density ρ_f. In work [27] it has been established that $\delta_f \approx 10^{-2}$ at high dislocation densities.

The analysis of published data concerning the reactions of dislocations in grain bodies and boundaries has shown that dislocation density decrease during the deformation can take place as a result of GBs "recovery" and annihilation of dislocations of opposite signs.

2.2.4. The annihilation of dislocations of opposite signs

By the beginning of stage II of deformation hardening the dislocation densities in primary and secondary slip systems become equal and increase dramatically along with strain [28]. This leads to annihilation of screw components of dislocation loops at low and moderate temperatures. By the beginning of stage III annihilation of screw dislocations is mainly due to cross slip [28]:

$$\frac{d\rho_{tot}^{-}}{dt} = -k_a \dot{\gamma}^r \rho_{tot}, \tag{20}$$

where k_a - the coefficient of annihilation of screw dislocations [29], $\dot{\gamma}$ - the rate of the plastic deformation. According to the experimental data [30,31], the annihilation coefficient k_a depends on the stacking fault energy and varies as 2÷10 in the case of FCC metals in the range of temperatures (0.1÷0.3) T_m (T_m is the melting temperature).

2.2.5. Grain boundaries recovery

Non-equilibrium GBs formed by SPD contain high density of extrinsic defects, have extra energy and long range elastic stress. These non-equilibrium GBs tend to a more stable state especially at elevated temperatures. Absorption of lattice dislocations by a grain boundary structure is one of the relaxation processes. The annihilation of edge dislocations in GBs is determined mainly by the time of pair annihilation of dislocations of opposite signs:

$$t_{gb} = \frac{kTd^2}{4D_{gb}Gb^3}, \tag{21}$$

The grain boundary diffusion coefficient $D_{gb} \approx 1.39\times10^{-20}$ m^{2}s^{-1} at T = 293K [5], T – the temperature. As a result, the dislocation density decreases with the rate

$$\frac{d\rho_{tot}^{-}}{dt} = -\frac{\rho_{tot}}{t_{gb}} = -k_{gb}\rho_{tot}\dot{\gamma}. \tag{22}$$

The annihilation coefficient here k_{gb} is determined as $k_{gb} = 1/t_{gb}\dot{\gamma}$.

In the model it was assumed that all the above mentioned processes take place independently. Then, their cooperative action leads to their linear addition in the equation of evolution of dislocation density, as it is described in work [21]. The equation describing change in the average dislocation density with strain $\gamma = M\varepsilon$ is given by [22]:

$$\frac{d\rho_{tot}}{d\gamma} = \frac{\beta}{bd} + \frac{1}{b\lambda_P} + \frac{1}{b\lambda_d} - k\rho_{tot}, \tag{23}$$

where $k=k_a+k_{gb}$.

3. THE RESULTS OF MODELING AND THEIR DISCUSSION

The reported experimental data [13] concerning Al-Mg alloys were used for modeling. A hot-pressed alloy Al 1570 annealed at 380 °C for 2 hours was considered as a CG state. For UFG states the annealed alloy was subjected to following HPT at RT (UFG state I), 100 °C (UFG state II), and 200 °C (UFG state III) (Table 1) [5]. Tensile tests were carried out at RT at a strain rate 10^{-4} s^{-1} [13].

Table 1. The values of the parameters, obtained experimentally in paper [13].

States	d, nm	ρ, m^{-2}	a, Å	σ_y, MPa	σ_u, MPA	δ, %
CG	$\approx 60\times10^3$	$\approx 1.0\times10^{11}$	4.0765±0.0001	231±9	376±10	17±1
UFGI	130±10	5.1×10^{14}	4.0692±0.0003	905±31	950±35	4.7±0,3
UFGII	130±10	3.4×10^{14}	4.0682±0.0002	865±25	890±18	4.0±0,4
UFGIII	210±7	5.6×10^{12}	4.0685±0.0001	845±33	845±33	0

The evaluations of the annihilation coefficient k_{gb} in case of UFG states carried out at d = 130 nm and d = 210 nm bring to values of 1.70 and 0.65 respectively. Estimation of the length of the free dislocation path λ_p for the CG state brings to values, which are one order less than the grain size, while the value λ_p is one order more in the UFG states. This means that dislocations will get the GBs faster, than their cross slip will happen. Thus, this mechanism of dislocation multiplication will not contribute into dislocation density accumulation in the UFG material. The corresponding estimations have shown that the dislocation multiplication mechanism on the forest dislocations does not contribute into dislocation accumulation both in the CG and in the UFG states [5]. During the calculations it has been accepted that $k_a \approx 2.1$ [21], $1/b\lambda_p \approx 59.4\times10^{13}$ $m^{-2}m^{-2}$, $\sigma_d \approx 220$ MPa.

In case of the CG Al 1570 alloy treated by heating up to 380 °C [13], when the atoms of alloying elements are well-distributed in a solid solution, while the dislocation density is 10^{11} m^{-2} [13], we consider that the offset yield strength is caused by the dislocation hardening σ_p, the solid solution hardening σ_c, the lattice resistance σ_0, hardening by the disperse particles σ_f:

$$\sigma_{0.2} = \sigma_0 + \sigma_c + \sigma_f + M\alpha Gb\rho^{1/2} = \sigma_d + M\alpha Gb\rho^{1/2}. \quad (24)$$

Additional hardening by Mg atoms with the increased concentration along the GBs is considered in the UFG state beside the action of the same hardening mechanisms as in CG state of the alloy. Under assumption of a dislocation passing from one boundary to another we consider that each dislocation has to overcome the increased concentration of Mg atoms and, hence, solute hardening is determined by this increased concentration: $\sigma_c^* = \sigma_c + \Delta\sigma_c$, where $\Delta\sigma_c$ is the extra stress due to Mg atoms along GBs area (it was considered that solid solution hardening is linearly proportional to solute atoms concentration: $\sigma_c = Kc$, K – the constant of proportionality).

Besides, as a result of HPT a high dislocation density has been accumulated in the UFG alloy, consequently, the contribution of dislocation hardening is characterized by the increased value.

As a result of the conducted experiments, the indications about the high level of inner stresses have been obtained, which could be the reason of segregations sinking along the GBs. The dislocations in the GBs area appear to be immersed into the solid solution with the increased concentration of Mg. As a result the dislocation displaced to some distance x from the impurity cloud will be affected by the increased power of dislocation pinning counted per unit of its length proportional to the impurity concentration in the area of 3 nm wide along the GBs [32]. As at a distance of 3 nm from dislocation the impurity atoms hardly feel the dislocation field and, consequently, the concentration of impurity atoms has little difference from the concentration in segregation, one can assume that the concentration of impurity atoms away from dislocation c_0 is equal to the increased concentration in the segregation.

Then, taking into consideration the hardening as a result of dislocation pinning $\sigma_s = M\tau_S$:

$$\sigma_{0.2} = \sigma_d + \sigma_s + \Delta\sigma_c + M\alpha Gb\rho^{1/2}. \quad (25)$$

It may be suggested that the stress value σ_d here is equal to the value, obtained in the equation (24), as the other mechanisms are calculated separately.

During HPT at RT, 100, and 200 °C about 1.59, 1.80 and 1.74 at.% Mg precipitated from the solid solution respectively. Mg atoms sink into the GBs area as it was proved by experimental observations [14,33]. As a result, atom concentration in GBs becomes equal to $\approx 98.37\times10^{26}$ m^{-3}, $\approx 149.53\times10^{26}$ m^{-3}, and $\approx 106.47\times10^{26}$ m^{-3} respectively. The pinning stress τ_S is then 106.4, 161.7, and 115.2 MPa, respectively [5] (Fig. 3).

The analysis of the modeling results demonstrates that high-strength states in the Al alloys subjected to HPT are caused by dislocation pinning by Mg atoms along GBs. The concentration of

Mg atoms in GBs increases, when the processing temperature increases from RT up to 100 °C under constant grain size. The stress of the dislocation pinning increases respectively. The obtained results are in agreement with the experimental data reporting segregations of Mg atoms along GBs [34,35].

As the number of β-phase particles appeared to be out of XRD limits [13], it can be assumed that Mg atoms stay mainly in the solid solution and form segregations along the GBs. In the annealed state of the alloy, Mg atoms are evenly distributed in the grain interior at Mg concentration of 5.7 wt.% (≈37.05×10^{26} m^{-3}).

The relative contribution of the above mentioned hardening factors into the investigated dependencies $\sigma = f(d^{-1/2})$ has been analyzed. The tendency of the alteration of the flow stress, conditioned by the microstructure imperfection depending on the grain size is presented (Table 2). The most defective is the UFG structure with d = 130 nm, obtained by HPT at room temperature. The less defective is the UFG structure with d = 210 nm obtained by HPT at 200 °C (Table 2). Correspondingly, the flow stress conditioned by the microstructure imperfection in the first case is higher than in the second one. At the same time the stress contribution of dislocation pinning by the Mg atoms in the GB area has the opposite tendency (Table 2).

The excess stress $\Delta\sigma_c$ is determined by subtraction from the experimental yield strength of the acquainted components of the theoretical flow strength. The deviation from the HP law of the Al 1570 alloy in the UFG state, as it has been suggested in paper [5], is mostly conditioned by the dislocation pinning by the Mg atoms. The concentration of Mg atoms as a result of HPT is high in the GBs area, which plays the principal role for the dislocation "sinks". Despite the high strength of the Al 1570 alloy with the grain size d = 130 nm, according to the obtained model, the flow stress could be higher, when the "grain reaches its maximum strength", the size of which is d_{cr}.

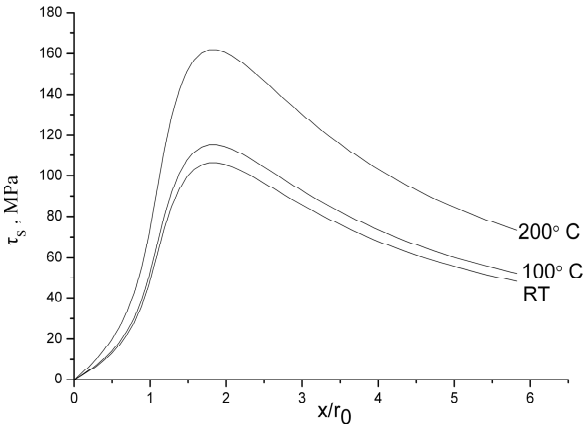

Fig. 3. The dependency of stress τ_S of the dislocation pinning from the value of dislocation displacement x from the fixed solute atmosphere.

We conclude that it is not proper to talk about alloys subjected to SPD in terms of the HP relationship. In such alloys "pumped up" by strengthening factors, special strengthening mechanisms act that are not typical for the CG materials. At the same time, the HP relation was established namely for these CG materials, which strength is mainly determined by limiting dislocation free path by GBs.

4. CONCLUSIONS

An analytical model that allows analyzing the deformation behavior of the alloys considering different deformation mechanisms has been developed. The equations of dislocation kinetics within the model take into consideration the possibilities of mechanisms of dislocation density increase as a result of the double cross slip, the limitation of the free dislocation path of GBs and deformation incompatibility, as well as mechanisms bringing to the decrease of dislocation density: annihilation of screw dislocations during the cross slip, relaxation of the non-equilibrium GBs.

With the aid of the model origins of the high-strength states in the UFG Al 1570 alloy subjected

Table 2. The values of experimental and calculated flow stress, as well as its components for CG and UFG states of the Al 1570 alloy.

Components of the Flow Limit	CG	UFG 1	UFG 2	UFG 3
Experimental Flow Limit $\sigma^{э}_{0,2}$, MPa	231±9	905±31	865±25	845±33
Theoretical Flow Limit $\sigma_{0.2}$, MPa	235.5	826	807	789
«Friction» of the lattice σ_d, MPa	220	220	220	220
Deformation hardening σ_ρ, MPa	15.5	279	233	73
Pinning Stress σ_s, mPa	–	327	354	496
Extra Solid Solution Hardening $\Delta\sigma_c$, MPa	–	79	58	56

to HPT at RT were analyzed. The components of the conventional flow stress of the alloy in the ÑG and UFG states have been calculated. It has been determined that additional hardening due to high concentration of Mg atoms along the GBs and increased value of work hardening play the key roles in the high strength of the UFG alloy. Both mechanisms are imposed by HPT. Since a number of strengthening factors take place in the UFG alloy that are not typical for CG state, it is not reasonable to apply the HP relation for the UFG state as the relation was obtained for a rather particular cases and under certain assumptions of CG polycrystals.

The quantitative evaluations of the dislocation pinning stress by the Mg atoms, precipitated from the solid solution of the alloy into the GBs, have been obtained as well as the stress, conditioned by the dislocation material hardening. The analysis of deformation mechanisms is reduced here too.

REFERENCES

[1] J.P. Hirth and J. Lothe, *Theory of dislocations* (Wiley, New York, 1982)

[2] J. Friedel, *Dislocations* (Pergamon Press, Oxford, 1964).

[3] J. Taylor // *J. Appl. Phys.* **36(10)** (1965) 3146.

[4] I.V. Alexandrov and R.G. Chembarisova // *Mater. Sci. Forum* **633-634** (2010) 231.

[5] I.V. Alexandrov and R.G. Chembarisova // *Rev. Adv. Mater. Sci.* **25** (2010) 209.

[6] I.V. Alexandrov and R.G. Chembarisova // *Mater. Sci. Forum* **667-669** (2011) 749.

[7] I.V. Alexandrov and R.G. Chembarisova // *Rev. Adv. Mater. Sci.* **16(1/2)** (2007) 51.

[8] Y. Estrin, L.S.Tóth, A. Molinari and Y. Bréchet // *Acta Mater.* **46** (1998) 5509.

[9] L.S. Tóth, A. Molinari and Y. Estrin // *J. Eng. Mater. Technol.* **124** (2002) 71.

[10] M. Zehetbauer // *Acta Mater.* **41** (1993) 589.

[11] P. Les, M. Zehetbauer // *Key Eng. Mater.* **97-98** (1994) 335.

[12] I.V. Alexandrov, R.G. Chembarisova and M.I. Latypov // *Mater. Sci. Forum* **683** (2011) 203.

[13] M.Yu. Murashkin, A.R. Kil'mametov and R.Z. Valiev // *The Phys. Met. Metallogr.* **106** (2008) 90.

[14] G. Nurislamova, X. Sauvage, M. Murashkin, R. Islamgaliev and R. Valiev // *Phil. Mag. Lett.* **88(6)** (2008) 459.

[15] I.P. Semenova, G.Kh. Salimgareeva, V.V. Latysh, T. Lowe and R.Z. Valiev // *Mater. Sci. Ing. A* **503** (2009) 92.

[16] R.L. Fleischer and W.R. Hibbard, In: *The Relation between the Structure and Mechanical Properties of Metals: Proceedings of the conference held at the National Physical Laboratory, Teddington, Middlesex on 7th, 8th and 9th January, 1963* (Her Majestry's Stationery Office: London, 1963), p. **452**.

[17] M. Phine, In: *Structure and Mechanical Properties of Metals* (Metallurgy, Moscow, 1967).

[18] I. I. Novikov, *The Defects of Crystalline Metal Structure* (Metallurgy, Moscow, 1983).

[19] M.A. Shtremel, *The Strength of Alloys. Part II. Deformation* (MISAA, Moscow, 1997).

[20] H. Konrad, In: *Ultrafine-Grain Metals*, ed. by John J. Burke and Volker Weiss (Syracuse University, Syracuse, 1973).

[21] U. F. Kocks and H. Mecking // *Progr. Mater. Sci*. **48** (2003) 171.

[22] G.A. Malygin // *Phys. Solid State* **49(6)** (2007) 1013.

[23] M.Yu. Gutkin, K.N. Mikaelyan and E.C. Aifantis // *Physics of the Solid State* **42** (2000) 1652.

[24] N.M. Vlasov // *Phys. of the Solid State* **43(11)** (2001) 2083.

[25] M.A. Shtremel, *The Strength of Alloys. Part I.The Lattice Faults* (Metallurgy, Moscow, 1982).

[26] A. Kelly, *Strong Solids, 2nd ed.* (Clarendon Press, Oxford, 1973).

[27] L.E. Popov, V.C. Kobytev and T.A. Kovalevskaya, *Plastic Deformation of the Alloys* (Metallurgy, Moscow, 1984).

[28] G.A. Malygin // *Phys. Solid State* **29** (1987) 1189.

[29] G.A. Malygin // *Phys. of the Solid State* **47** (2005) 246.

[30] G.A. Malygin // *Phys. Solid State* **37** (1995) 1.

[31] G.A. Malygin // *Physical Science Success* **169(9)** (1999) 979.

[32] R.Z. Valiev, R.K. Islamgaliev and I.V. Alexandrov // *Progr. Mater. Sci*. **45** (2000) 103.

[33] *Aluminum: Properties and Physical Metallurgy*, ed. by J. E. Hatch (AMS, Metals Park: Ohio, 1984; Metallurgy: Moscow, 1989).

[34] T. Fujita, Z. Horita and T.G. Langdon // *Philos. Mag. A* **82(11)** (2002) 2249.

[35] L.N. Gusev, M.F. Nikitina, L.D. Dolinskaya and I.V. Egiz // *Izv. Akad. Nauk SSSR, Met*. **4** (1972) 208.